Available online at www.sciencedirect.com

ScienceDirect

journal homepage: http://www.elsevier.com/locate/acme

Review

Chemical polishing of scaffolds made of Ti–6Al–7Nb alloy by additive manufacturing

E. Łyczkowska *, P. Szymczyk [1], B. Dybała [2], E. Chlebus [3]

Wrocław University of Technology, Faculty of Mechanical Engineering, CAMT – FPC, 5 Łukasiewicza Street, 50-371 Wrocław, Poland

ARTICLE INFO

Article history:
Received 9 April 2013
Accepted 9 March 2014
Available online 5 April 2014

Keywords:
Chemical polishing
Selective laser melting
Scaffold
Titanium alloy Ti–6Al–7Nb

ABSTRACT

The titanium–aluminium–niobium alloy is used in bone, dental and articular prosthetics, where high final surface quality is required. Bone scaffolds for tissue engineering require optimized cellular structures to provide pore diameters allowing the growth of osteoblasts. The aim of the presented paper is to estimate the quality of surface treatment of components with complex spatial structure, made of Ti–6Al–7Nb alloy by powder-bed selective laser melting (SLM), which is one of the additive manufacturing technologies for metal materials. Test pieces were subjected to chemical polishing to improve surface quality and remove loose powder particles trapped in the porous structure. It was found that resulting surface roughness and reduction of the number of non-melted powder particles on the scaffold surface are influenced mostly by chemical composition and concentration of the bath, as well as the method of medium delivery and exchange during the process. Further investigations were aimed at optimizing the process and increasing the number of workpieces processed in a single lot.

1. Introduction

Titanium and its alloys are widely applied in many fields of life. Besides aluminium and magnesium, titanium is the third (with density of 4.51 g/cm^3) light metal, widely used for structures in aircraft, automotive and aerospace industries, as well as in competitive sport, jewellery and biomedical engineering. Depending on temperature, titanium exists in two allotropic forms: low-temperature α and high-temperature β. The α form is stable up to 882 °C and crystallizes in the hexagonal close-packed (HCP) lattice, and the β form is stable

* *Corresponding author at*: CAMT, Centre for Advanced Manufacturing Technologies, ul. Lukasiewicza 5, 50-371 Wroclaw, Poland. Tel.: +48 071 320 20 44.
E-mail addresses: edyta.lyczkowska@pwr.wroc.pl (E. Łyczkowska), patrycja.e.szymczyk@pwr.wroc.pl (P. Szymczyk), bogdan.dybala@pwr.wroc.pl (B. Dybała), edward.chlebus@pwr.wroc.pl (E. Chlebus).
[1] CAMT, Centre for Advanced Manufacturing Technologies, ul. Lukasiewicza 5, 50-371 Wroclaw, Poland. Tel.: +48 071 320 20 74.
[2] CAMT, Centre for Advanced Manufacturing Technologies, ul. Lukasiewicza 5, 50-371 Wroclaw. Tel.: +48 071 320 50 04; fax: +48 071 328 06 70.
[3] CAMT, Centre for Advanced Manufacturing Technologies, ul. Lukasiewicza 5, 50-371 Wroclaw, Poland. Tel.: +48 071 320 20 75.
http://dx.doi.org/10.1016/j.acme.2014.03.001

from 882 °C up to the melting point of 1668 °C and crystallizes in the body-centred cubic (BCC) lattice. A representative of the alloys used so far in medicine is Ti–6Al–4V with two-phase $\alpha + \beta$ structure, characterized by high strength and fracture toughness. Because of good mechanical properties, it is also applied in heavy industry for manufacturing of components of power units and airframes [8,15,16,19,26]. The Ti–6Al–7Nb alloy is a new-generation material that, unlike the alloys used so far, does not contain vanadium, thanks to that it can find application in implantology. Niobium that substitutes vanadium in this alloy improves properties of its biomedical application [12].

Titanium is a highly reactive metal, able to create a stable passive layer in form of titanium oxide ca. 2–5 nm thick that protects the material against external factors (air and water). The protective layer of titanium oxide on an implant surface permits complete integration with human tissue (passive TiO layers are neutral for human organism) [4,20]. Titanium alloys are used in implant manufacturing because of their bioacceptability, beneficial mechanical properties (Young's modulus comparable to that of bones) and fatigue strength dependent on presumed applications [6,7,13,22]. Thanks to high bioacceptability, titanium and its alloys can be used for long-term implants, whose working life in a human body can reach several years. An important feature of titanium alloys is their osteointegration capacity [1].

Machining of titanium and its alloys with traditional methods causes many difficulties of both technical and economic nature. In case of mechanical grinding of a titanium alloy, a low metal removal rate with considerable wear of the grinding wheel is usually obtained. For many years searched have been possibilities of increasing efficiency of machining titanium alloys with traditional methods, as well as new machining methods, like chemical and electrochemical polishing or electrochemical-abrasive machining [25]. Machinability of titanium and its alloys is considered as bad because of a tendency to build-up on the tool edge, low thermal conductivity leading to high temperature during machining, and a tendency for strain hardening in the machining area. This specificity of machining is manifested by high force and torque values, as well as extremely high thermal loads of cutting edges, which results in intensive wear and deformation of the tools [14].

Implants made of titanium alloys can be used in tissue engineering as cell scaffolds for treating large cavities in bones [2,9], created as a result of injury or disease processes [7]. Scaffolds' porous structure improves implant-bone joints, supports links between the implant surface and osteoblasts and allows for extensive transport of body fluids within the implant-tissue complex. The porous structure must constitute scaffolding for the cells during in vitro breeding and suppress external loads after in vivo implantation [10,22]. The scaffolds having pores with relatively large diameter permit better interaction of cells with growth factors and other ligands that affect functions and differentiation of cells.

For constructions with complex internal structures, manufacturable with powder-based additive technologies like SLM, mechanical working (machining or vibro-abrasive machining) is unable to ensure the desired surface smoothness and to remove loose powder particles left after the build processes. In case of tiny open-work structures, applied in tissue engineering, it is possible to form the surface using chemical and electrochemical methods. It is important that the process should be well controlled to ensure obtaining the surface topography with required properties. For initial and final treatment of the objects produced by traditional and additive methods, the process of chemical polishing can be used, during which a surface layer is created on the polished metal. The diffusive layer is water-deficient in the pits, so the metal is faster dissolved on the peaks [3]. The process of chemical polishing titanium alloys can employ baths containing hydrofluoric acid and nitric acid [5].

Methods of chemical polishing of metal scaffolds described by other authors [9,10,22] concern additively manufactured structures with pore sizes exceeding 800 μm. We focused on optimization of chemical polishing of samples with smaller-scale structures, with pores in the range of 400 μm. Our research also covered series of samples where we designed a method of processing up to 10 scaffolds and proved that increasing the number of workpieces in a processed lot does not influence processing results in a significant way.

In the SLM technology components are manufactured using a focused laser beam that selectively melts powder material applied in layers on the working platform, see Fig. 1a. The component layers are built of newly applied powder fed from

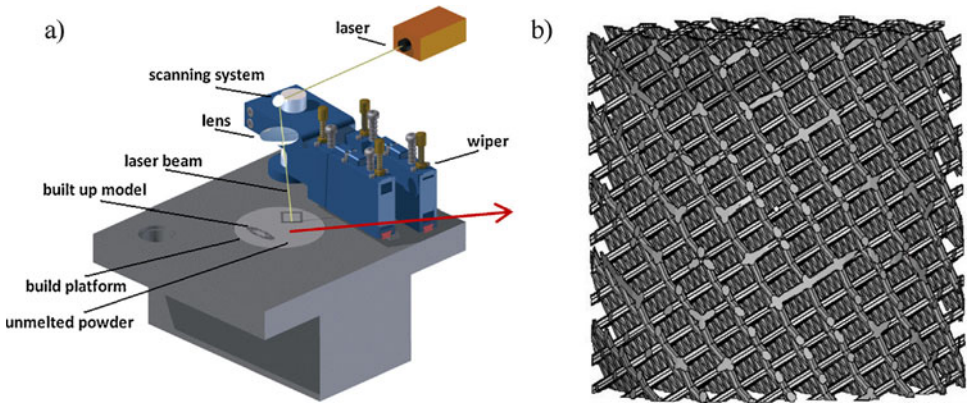

Fig. 1 – (a) Layout of the SLM equipment [6]. (b) CAD model of a sample.

Table 1 – Technological parameters used to build the test pieces.

Parameter	Value
Laser power	25 W
Layer thickness	50 μm
Scan velocity	0.2 m/s
Scanning strategy	Double x–y

a moving container and overlapped on the previous layers, which ensures durable bonding within the entire model. The SLM technology gives possibilities to produce homogeneous new-generation implants (scaffolds) characterized by high manufacturing accuracy. This technology makes it possible to reduce the mass of a component (up to 80%), to modify its stiffness (comparable with stiffness of the bone to be replaced) and to create space for growing cells that support osseointegration [23,24]. Changes of the surface topography can attribute to rejecting a scaffold due to its high cytotoxicity and therefore it is important to prepare the surface preliminarily, before applying a hydroxyapatite layer to improve biocompatibility. Forming the properties of the surfaces made by SLM still presents a technological problem. With respect to the process specificity, the SLM technology generates some restrictions. Shape of individual grains must ensure proper liquidity of powder during applying individual layers and permit maintaining geometry of each single cross-section during remelting the powder.

2. Materials and methods

2.1. *Fabrication of samples*

For the presented investigations, cellular matrix with unit cell size 600 μm and struts of 250 μm thickness were built using the SLM technology, based on a designed CAD model (Fig. 1b).

The technological parameters used at building the test samples by SLM are shown in Table 1.

Scaffolds were made of titanium alloy Ti–6Al–7Nb powder with particle size smaller than 63 μm. Particles were separated by sieve analysis (acc. to EN 24497/ISO 4497). Examination of titanium alloy particles using scanning electron microscopy revealed their regular (spheroidal) shape (Fig. 2a) that is beneficial for proper powder flow in the SLM process.

Table 2 – Chemical composition of processed Ti–6Al–7Nb powder.

Element	Actual concentration (wt%)	Requirements of ISO 5832-11 (wt%)
Ti	Rem.	Rem.
Al	5.74	5.50–6.50
Nb	6.50	6.50–7.50
Fe	0.047	<0.25
C	0.011	<0.08
Ta	<0.001	<0.50

The chemical composition of powder was determined by the spectroscopy method according to the ISO 5832-11 standard, results are given in Table 2.

The example of a scaffold produced by SLM is shown in Fig. 2b. Dimensions of the finished scaffolds were: diameter 6.2 mm and 6.0 mm height. The internal structure of the manufactured samples was fully homogeneous, consisting of elementary cubes with 12 orthogonal struts.

The average diameter of scaffold struts after the SLM process, measured by a scanning electron microscope, was 242 μm and the average mass of the specimens was 0.215 g. The scaffolds were chemically polished in a bath consisting of hydrofluoric acid, nitric acid and water.

2.2. *Chemical polishing*

The scaffolds were chemically polished in the baths consisting of 80 vol% H_2O, 6 vol% HF and 14 vol% HNO_3 [5] or of 99 vol% H_2O and 1 vol% HF [9–11,22]. Before polishing, specimens were subject to preliminary cleaning in an ultrasonic cleaner containing first distilled water and then ethanol.

The first lot of the workpieces was chemically polished in the ultrasonic cleaner and the second lot was stirred with a magnetic stirrer. Times of polishing were 60, 80, 90, 600, 700

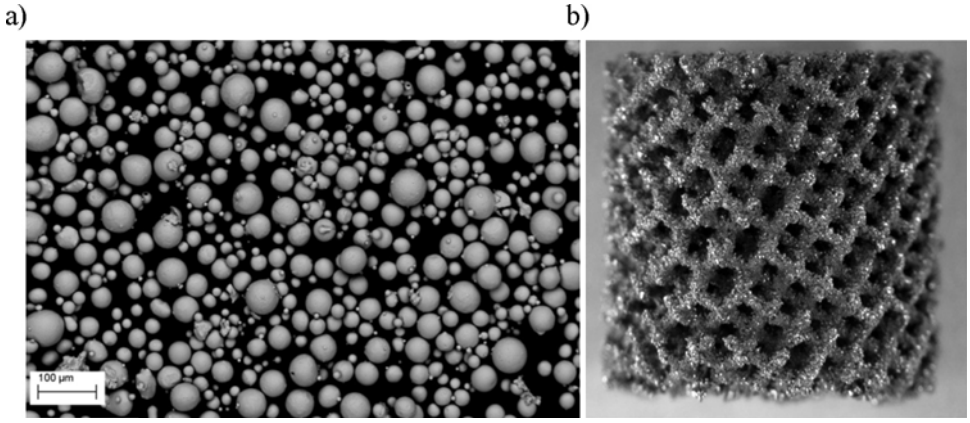

Fig. 2 – (a) Particles of Ti–6Al–7Nb powder, SEM. (b) Scaffold made of Ti–6Al–7Nb alloy by the SLM technology [21] – cylinder diameter of 6.2 mm, 6 mm high, light microscope.

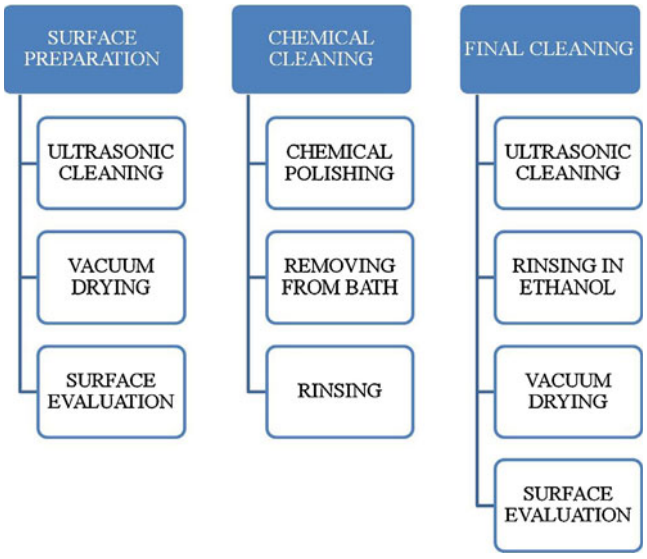

Fig. 3 – Technological diagram of chemical cleaning process.

and 900 s, counted from dipping the scaffolds in the baths. After chemical polishing, the specimens were again rinsed and dried.

On the grounds of obtained results, the most favourable bath and the most favourable way of stirring were chosen. A positive result of smoothing the surface was obtained after three process stages:

(1) surface preparation (removing dust and loose powder particles that could disturb chemical polishing);
(2) chemical polishing;
(3) final cleaning (removing bath residues and drying the metal surface).

The entire polishing process is schematically shown in Fig. 3.

The scaffolds were next subject to micro-computed tomography (METROTOM 1500) to estimate their geometry and shape. To achieve high resolution, the tube voltage was fixed at the level of 220 kV and the current at 120 μA, the number of projections was 800 with 1 s integration time.

Observations were also carried-out using a scanning electron microscope ZEISS EVO MA 25. The examinations were aimed at evaluating surface quality of the produced scaffolds directly after the SLM process and after additional chemical polishing, as well as at determining intensity of chemical polishing on changes of weight and reduction of strut diameters in relation to the initial conditions.

2.3. *XPS investigations*

The chemical composition of the surfaces was determined by XPS (X-ray photoelectron spectroscopy), using a SPECS UHV system equipped with a PHOIBOS 100 spectrometer and SpecLab software. XPS investigations were performed on samples before and after chemical polishing (times of 600 and 1200 s were used). Three series of XPS investigation at different heights of samples were made. There were two steps of Ar^+ etching. The parameters of every step were 3 keV and 5–6 μA/cm^2. Etching with Ar^+ helped remove carbon compounds from the analyzed surface. The intensity of the one step etching was less than 20–30 nm.

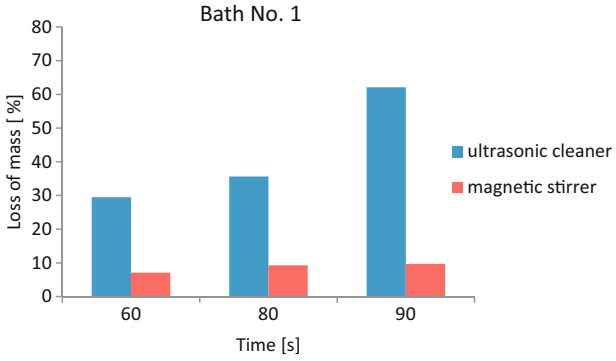

Fig. 4 – Loss of mass of the specimens polished in an ultrasonic cleaner and using a magnetic stirrer.

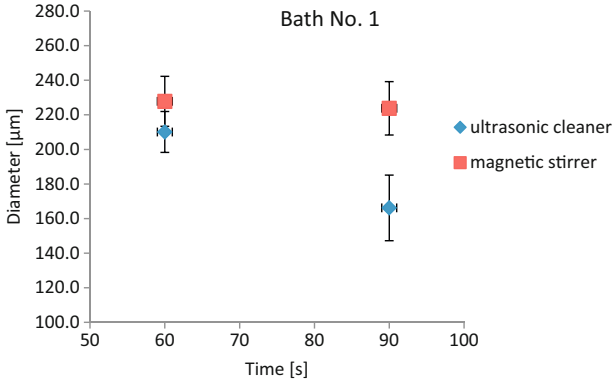

Fig. 5 – Strut diameter of the specimens polished in an ultrasonic cleaner and using a magnetic stirrer.

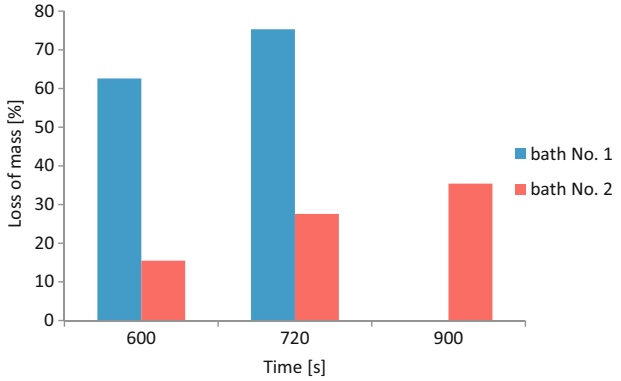

Fig. 6 – Loss of mass of the specimens polished in baths with various composition, using a magnetic stirrer.

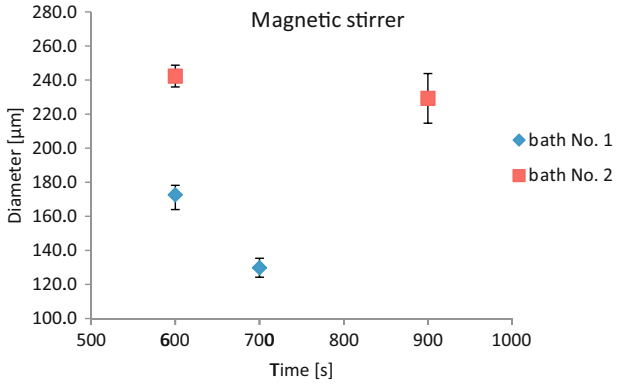

Fig. 7 – Strut diameter of the specimens polished in baths with various composition, using a magnetic stirrer.

3. Results

3.1. *Chemical polishing*

Samples were manufactured by selective laser melting, from Ti–6Al–7Nb powder. They were cylindrical in shape and had internal structure as described in Section 2.1. Loss of mass and strut diameter after chemical polishing in an ultrasonic cleaner and using a magnetic stirrer are shown in Figs. 4 and 5, respectively.

Loss of mass and volume of the scaffolds polished in the ultrasonic cleaner was much larger than those of the specimens polished using the magnetic stirrer. Moreover, in the first case, some over-polished areas could be observed – the scaffold surface was too intensively polished, see Fig. 11. It was found that the process carried out in the ultrasonic cleaner is unstable and difficult to be controlled.

Fig. 6 shows loss of mass of the specimens polished in baths with various compositions: bath no. 1 and bath no. 2.

The specimens polished in the bath consisting of distilled water with an addition of hydrofluoric acid had regular surfaces. Reducing acid concentration in the bath and extending the immersion time instead, resulted in the absence of large cavities caused by more concentrated baths and still successful removal of partially bound, non-melted powder particles (Fig. 7).

Fig. 8 shows a scaffold before chemical polishing. In the magnified view partially bound Ti–6Al–7Nb powder particles are visible left after the SLM process.

Results of chemical polishing after 600 s in the bath no. 2 using the magnetic stirrer are shown in Fig. 9. Surfaces of the struts are more uniform, almost no semi-attached powder particles remain.

The analysis carried out by micro computed tomography (µCT) for samples described above, confirmed the effectiveness of the chemical polishing process. The samples polished in bath no. 1 exhibit a distinct decrease in volume after the polishing process, see Fig. 10b. Cross-sections made through

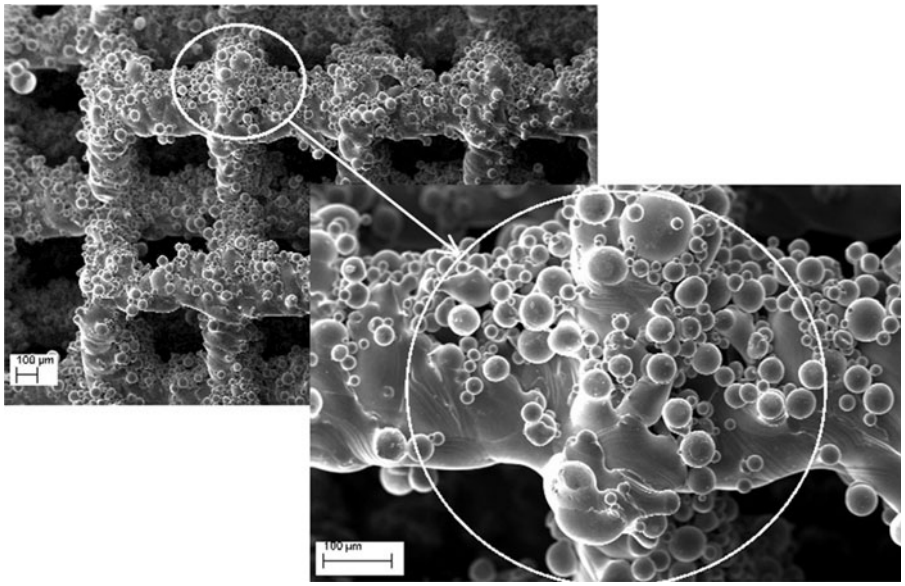

Fig. 8 – Scaffold before polishing. Partially bound powder particles on a strut surface visible in the magnified image.

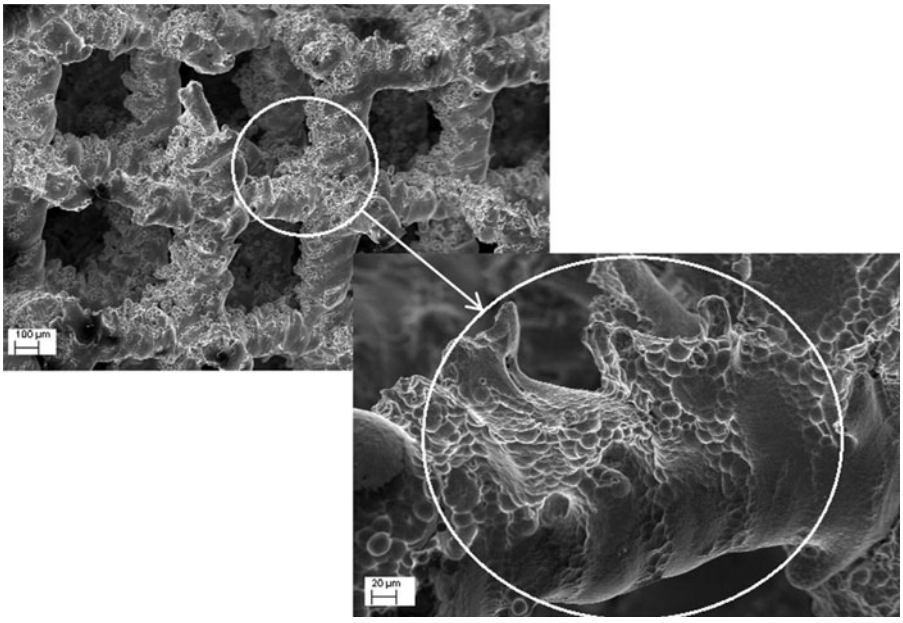

Fig. 9 – Scaffold after polishing for 600 s in bath no. 2 (magnified strut surface).

the test structures have shown that the loss of volume is uniform throughout the sample.

After optimizing the process, i.e. choosing a bath, a polishing method and a processing time, examinations were carried-out in order to increase the size of the process lot and to reduce the time of processing larger numbers of scaffolds. A special basket containing 20 pockets for workpieces was prepared, assuring the same bath conditions for all samples.

Table 3 shows results of polishing various numbers of cylindrical scaffolds in a lot. It was found that size of a lot does not significantly affect processing results.

3.2. *XPS investigations*

The XPS spectra for scaffold samples are presented in Fig. 12. A wide range of elements can be recognized here (Ti, Nb, Al, C, O, and F). Table 4 shows the chemical composition of Ti–6Al–7Nb surface of the investigated samples after SLM process. The results of XPS analysis after chemical polishing of samples in bath no. 2 are presented in Table 5.

Carbon pollutions on the surface are likely the effect of washing the samples in ethanol. Fluorine components are located on the surface of the polished samples and tightly

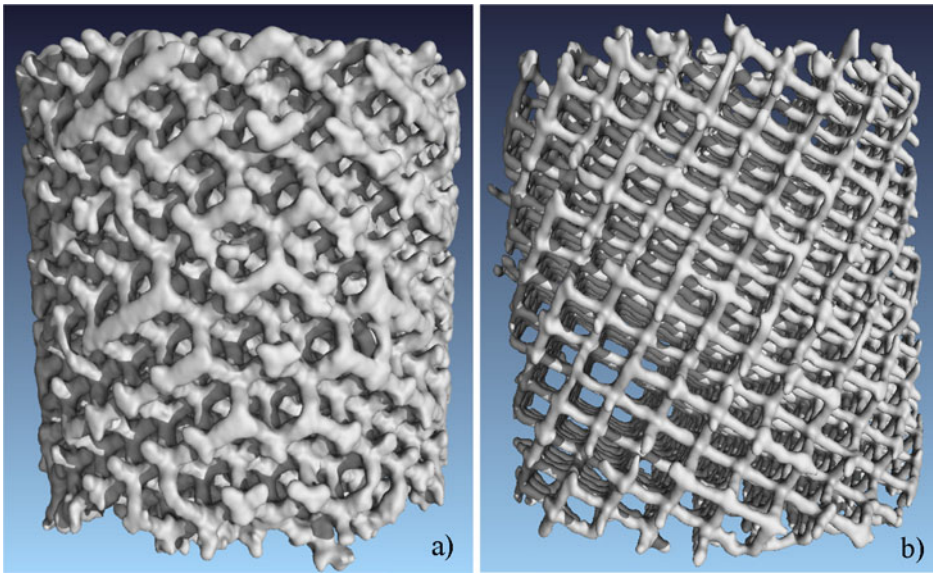

Fig. 10 – 3D reconstruction of scaffold structures: (a) before chemical polishing and (b) after chemical polishing (bath no. 1) – visible identical sizes of struts, µCT [21].

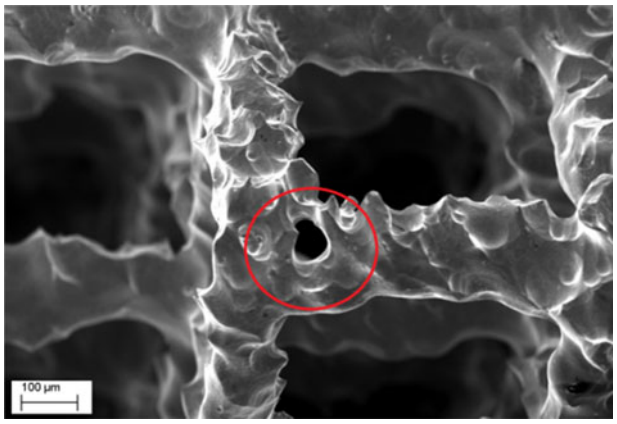

Fig. 11 – Scaffold after polishing for 90 s in bath no. 1. A damaged place (over-polished) is marked with a circle.

Table 3 – Loss of mass depending on the number of cylindrical scaffolds in a lot.

Lot no.	Number of workpieces in a lot	Loss of mass (wt%)
1	1	22.4
2	1	
3	1	
4	1	
5	1	
6	3	20.7
7	3	
8	3	
9	5	21.9
10	5	
11	5	
12	8	20.2
13	8	
14	10	21.2

Table 4 – The chemical composition of Ti–6Al–7Nb sample surface (at%) by XPS, before and after steps I and II of Ar^+ etching.

Etching	C	N	O	Al	Nb	Ti
None	24.1	4.4	50.3	4.7	0.3	16.2
I	8.0	12.2	49.7	5.2	0.6	24.3
II	7.0	14.9	45.4	4.2	0.6	27.9

bound with the surface. Titanium is mostly present in the form of TiO_2. Fig. 13a shows two peaks at the binding energies of 459.5 eV (Ti $2p_{3/2}$) and 465 eV (Ti $2p_{1/2}$). A similar situation can be observed for niobium. The peaks at 208 (Nb $3d_{5/2}$) and 210.5 eV (Nb $3d_{3/2}$) show the presence of Nb_2O_5, Fig. 13b [18,19]. The binding energy of the fluorine compounds with titanium is higher than in TiO_2, because of the remarkable electronegativity of fluorine. After chemical polishing fluorine compounds of titanium, niobium or aluminium may form on the surface. Fig. 13c shows the fluorine peak (F 1s) at 685.7 eV which can be the hexafluorotitanate complex $[TiF_6]^{2-}$ [17]. The fluorine to titanium ratio is higher on the surface after chemical polishing than after chemical polishing and Ar^+ etching. The at% ratio of the fluorine to titanium concentration on the surface of the samples gradually decreases from 0.209 to 0.099 after second Ar^+ etching of samples polished for 1200 s in bath no. 2. The higher quantity of fluorines on the surface is the result of chemical polishing in the bath consisting of hydrofluoric acid. The lower quantity of aluminium on the surface can be connected with fluorine compounds which are reacting most likely first with the aluminium and then with titanium and niobium. After Ar^+ etching, we see a peak for aluminium at 74.4 eV (Al 2p), Fig. 14. The spectra do not show peaks at lower energies, characteristic for metallic titanium and niobium on surfaces without Ar^+ etching, which suggest that the thickness of the oxide layer is at least a few nanometers.

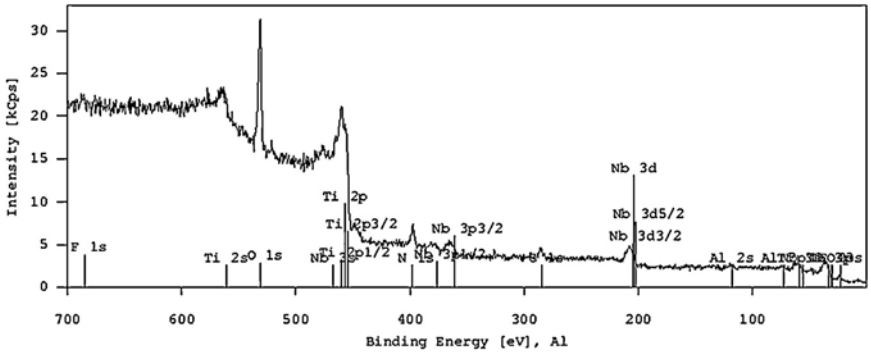

Fig. 12 – The XPS spectra of chemical polished Ti–6Al–7Nb samples polished for 1200 s in bath no. 2.

Table 5 – The chemical composition of Ti–6Al–7Nb sample surface after chemical polishing of different durations (at%) by XPS, before and after steps I and II of Ar^+ etching.

Time (s)	Etching	C	N	O	F	Al	Nb	Ti	F/Ti
600	None	27.6	8.8	43.8	1.5	2.6	2.2	13.5	0.111
	I	10.7	13.6	44.6	1.9	2.1	2.6	24.6	0.077
	II	8.1	13.8	45	2.2	3.4	2.1	25.4	0.087
1200	None	27.7	7.9	45.1	2.9	–	2.4	13.9	0.209
	I	12.2	12.3	44.6	3	–	2.6	25.3	0.119
	II	6.9	12.9	46.9	2.5	2.2	3.3	25.2	0.099

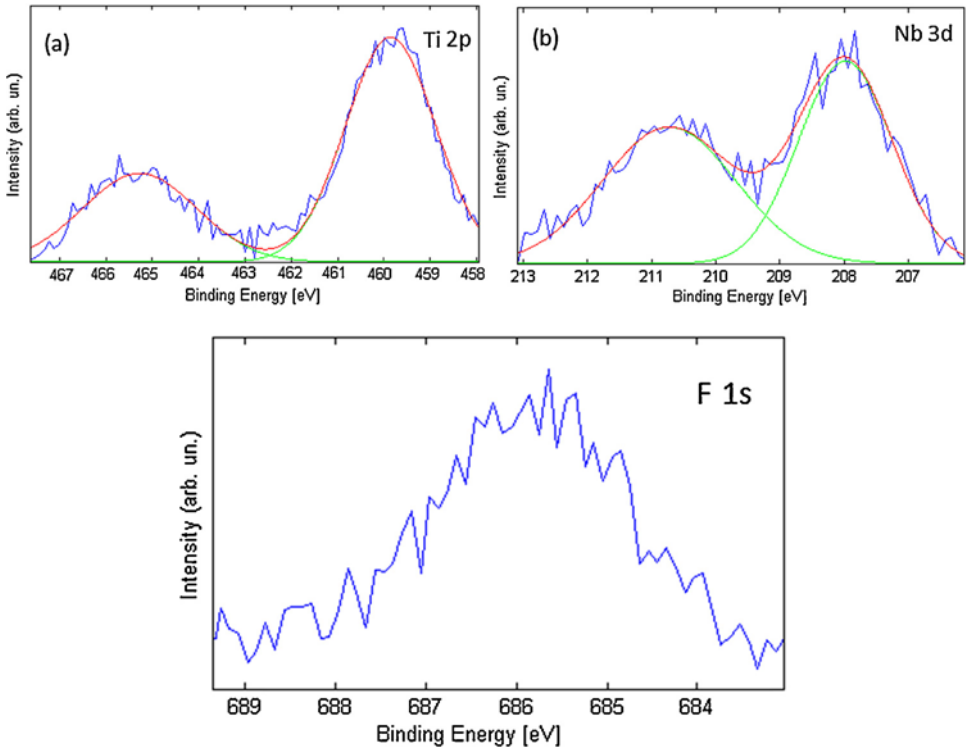

Fig. 13 – The Ti2p, Nb3d, F1s fitted spectra of Ti–6Al–7Nb alloy samples polished for 1200 s in bath no. 2.

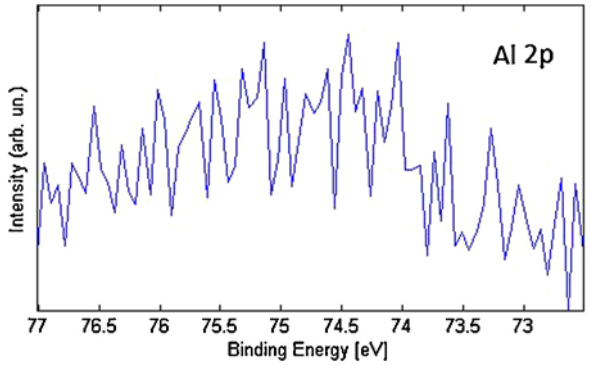

Fig. 14 – Al2p fitted spectra of Ti–6Al–7Nb alloy samples polished for 1200 s in bath no. 2, after steps I and II of Ar^+ etching.

4. Conclusions

The presented method allows for chemical polishing of surfaces of tissue scaffolds made by the SLM technology. The described examinations clearly demonstrate a relationship between the process parameters, i.e. polishing time and composition of the bath, and the loss of mass of polished workpieces. The loss of mass is related to removing partially bound, non-melted powder particles from surfaces of the struts and also to reducing their diameters. A significant reduction of the bath concentration together with extension of the processing time permits removing the partially bound particles and reducing surface roughness that is left in the case of using the more concentrated bath. Longer time of chemical polishing in less concentrated bath permits better process control and thus obtaining more repeatable results. Polishing using a magnetic stirrer ensures greater stability of the process.

The method may be used for treatment of small-scale structures, with pores in the range of 400–420 μm. Our investigations also covered batch treatment – we designed a method of processing up to 10 scaffolds and proved that increasing the number of workpieces in a processed lot does not significantly influence results.

In a further research, the chemical bath should be modified by adding oxidants and the process of electro-polishing should be applied in order to create a passive layer on the workpiece surface.

Acknowledgements

Authors wish to thank for the financial support from the project "*Bio-implants for osseous tissue decrement in patients with cancer treatment*" (contract number POIG.01.01.02-00-022/09; co-funded by the European Regional Development Fund).

REFERENCES

[1] J. Adamus, M. Gierzyńska-Dolna, Titanium and modern material used for implants, Inżynieria Materiałowa 3 (2012) 189–192.

[2] K. Alvarez, H. Nakajima, Metallic scaffolds for bone regeneration, Materials 2 (2009) 790–832.
[3] S. Bagdach, et al., Poradnik galwanotechnika, Scientific Publishing House PWN, Warsaw, 1994.
[4] M.A. Birch, S.S. Johnson-Lynn, Q.-B. Nouraei Wu, S. Ngalim, W.-J. Lu, C. Watchorn, T.-Y. Yang, A.W. McCaskie, S. Roy, Effect of electrochemical structuring of Ti6Al4V on osteoblast behaviour in vitro, Biomedical Materials 7 (2012) 1–14.
[5] Chemical and Electrolytic Polishing, Metallography and Microstructures, vol. 9, ASM Handbook, ASM International, 2004.
[6] E. Chlebus, B. Kuźnicka, T. Kurzynowski, B. Dybała, Microstructure and mechanical behaviour of Ti–6Al–7Nb alloy produced by selective laser melting, Materials Characterization 62 (2011) 488–495.
[7] B. Dąbrowski, W. Święszkowski, D. Godliński, K.J. Kurzydłowski, Highly porous titanium scaffolds for orthopaedic applications, Journal of Biomedical Materials Research Part B: Applied Biomaterials 95B (2010) 53–61.
[8] W. Grzesik, J. Małecka, Machining of titanium and Ti–Al alloys based on intermetallic phases, Nowe Technologie (2011) 136–142.
[9] G. Kerckhofs, S. Van Bael, G. Pyka, J. Schrooten, M. Wevers, Investigation of the influence of surface roughness modification of bone tissue engineering scaffolds on the morphology and mechanical properties, in: SkyScan User Meeting, Mechelen, Belgium, (2010), pp. 1–5.
[10] G. Kerckhofs, S. Van Bael, G. Pyka, J. Schrooten, M. Moesen, D. Loeckx, M. Wevers, Non-destructive characterization of the influence of surface modification on the morphology and mechanical behavior of rapid prototyped Ti6Al4V bone tissue engineering scaffolds, in: European Conference for Non-Destructive Testing (ECNDT), vol. 10, Moscow, Russia, (2010), pp. 1–9.
[11] J.D. Lee, Zwięzła chemia nieorganiczna, Scientific Publishing House PWN, Warsaw, 1994312–318.
[12] M.F. López, A. Gutierrez, J.A. Jimenez, In vitro corrosion behaviour of titanium alloys without vanadium, Electrochimica Acta 47 (2002) 1359–1364.
[13] C. Madore, D. Landolt, Electrochemical micromachining of controlled topographies on titanium for biological applications, Journal of Micromechanics and Microengineering 7 (1997) 270–275.
[14] K.E. Oczoś, Machining of titanium and its alloys in aircraft industry and medical technology, Mechanik 8–9 (2008) 639–656.
[15] K.E. Oczoś, Machining of titanium and its alloys in aircraft industry and medical technology, Mechanik 10 (2008) 753–767.
[16] R. Orlicki, B. Kłaptocz, Titanium and its alloys – properties, application in dentistry and processing methods, Inżynieria Stomatologiczna Biomateriały 1 (2005) 4–9.
[17] D. Regonini, A. Jaroenworaluck, R. Stevensa, C.R. Bowena, Effect of heat treatment on the properties and structure of TiO_2 nanotubes: phase composition and chemical composition, Surface and Interface Analysis 42 (2010) 139–144.
[18] W. Simka, M. Mosiałek, G. Nawrat, P. Nowak, J. Żak, J. Szade, A. Winiarski, A. Maciej, L. Szyk-Warszyńska, Electrochemical polishing of Ti–13Nb–13Zr alloy, Surface & Coatings Technology 213 (2012) 239–246.
[19] W. Simka, G. Nawrat, J. Chłodek, A. Maciej, A. Winiarski, J. Szade, K. Radwański, J. Gazdowicz, Electrolytic polishing and anodic passivation of Ti–6Al–7Nb alloy, Przemysł Chemiczny 90 (2011) 84–90.
[20] C. Sitting, M. Textor, N.D. Spencer, M. Wieland, P.H. Vallotton, Surface characterization of implant materials c.p. Ti, Ti–6Al–7Nb and Ti–6Al–4V with different pretreatments, Journal of Materials Science: Materials in Medicine 10 (1999) 35–46.
[21] P. Szymczyk, A. Junka, G. Ziółkowski, M. Bartoszewicz, E. Chlebus, The ability of *S. aureus* to form biofilm on the Ti–6Al–7Nb scaffolds produced by selective laser melting and subjected to the different types of surface modifications, Acta of Bioengineering and Biomechanics 15 (2013) 69–76.
[22] S. Truscello, G. Kerckhofs, S. Van Bael, G. Pyka, J. Schrooten, H. Oosterwyck, Prediction of permeability of regular scaffolds for skeletal tissue engineering: a combined computational and experimental study, Acta Biomaterialia 8 (2012) 1648–1658.
[23] M. Wehmöller, P.H. Warnke, C. Zilian, H. Eufinger, Implant design and production – a new approach by selective laser melting, International Congress Series 1281 (2005) 690–695.
[24] T. Wohlers, Report 2009, State of Industry, Annual Worldwide Progress Report, Wohlers Associates Inc., Colorado, 2009.
[25] S. Zaborski, M. Łupak, D. Poroś, Oxide layer on the surface of titanium alloy WT3-1 created during electrochemical-abrasive machining, Przegląd Mechaniczny 11 (2005) 25–29.
[26] L. Xuanyong, K. Chub Paul, C. Dinga, Surface modification of titanium, titanium alloys, and related materials for biomedical applications, Materials Science and Engineering 47 (2004) 49–121.